Hydrodynamic sound experiments in normal and superfluid ^{3}He

G. Eska, K. Neumaier, W. Schoepe,* K. Uhlig, and W. Wiedemann
Zentralinstitut für Tieftemperaturforschung, D-8046 Garching, Federal Republic of Germany
(Received 15 July 1982; revised manuscript received 7 January 1983)

In a cylindrical resonator the attenuation and the velocity of first sound in normal and superfluid ^{3}He have been measured in the frequency range from 40 to 300 kHz and at pressures of 8, 18.8, and 28 bar. In the normal fluid the viscosity deduced from our data agrees with previously reported values; the sound velocity in this regime can be explained by taking into account mean-free-path effects and zero-sound corrections. The results for the viscosity in the superfluid confirm the previous observations of a continuous decrease down to the lowest temperatures in contradiction to theoretical predictions. The sound-velocity data in the superfluid regime indicate that specular reflection of the quasiparticles may occur at the resonator walls.

I. INTRODUCTION

After the discovery of the superfluid phases of ^{3}He by Osheroff, Richardson, and Lee in 1971,[1] many attempts have been made to determine the viscosity of the superfluid. While the normal-fluid viscosity of ^{3}He is well understood, there are still discrepancies between the various experiments and theories in the superfluid regime. Until now η and the normal-fluid density ρ_n have been determined by using vibrating-wire viscometers[2,3] or torsional oscillators.[4,5]

The most extensive measurements of viscosity and normal-fluid density in superfluid ^{3}He were reported by Archie *et al.*[6,7] They used both a vibrating-wire viscometer and a torsional pendulum. These two viscometers gave the same result: a rapidly dropping viscosity below the transition temperature T_c followed by a slower but still monotonic decrease down to their lowest temperature $T=0.4T_c$. Recently, the same behavior was found by Carless *et al.*[8] down to $T=0.25T_c$ where η was only $0.03\eta(T_c)$.

Thus, with the exception of the first experiments of Alvesalo *et al.*,[2] all further experiments showed this continuously decreasing viscosity in the whole temperature regime investigated. This is in clear contradiction to theoretical calculations[9–12] that predict temperature independence and a finite value of η at low temperatures.

The present work was carried out in order to help clarify this situation by using a completely different experimental method, namely the attenuation of hydrodynamic (first) sound in a cylindrical resonator, which makes it possible to measure simultaneously both the sound absorption and the sound velocity at different frequencies (harmonics of the fundamental plane-wave resonance of the resonator). From the sound attenuation α we calculate the shear viscosity η. At the same time the sound velocity c_1 is derived from the frequency of the sound waves. At low temperatures and high frequencies, corrections to the hydrodynamic theory due to the increase in the collision time of the quasiparticles are not negligible anymore. In this regime the quasiparticle mean free path becomes comparable to the viscous penetration depth δ; this gives rise to a slippage of the fluid at the resonator walls. Both the sound attenuation α as well as the sound velocity c_1 are affected by the "slip effect." In this paper we report on the first measurements of this effect in the liquid ^{3}He. There are also corrections to the bulk behavior due to the beginning transition to the zero-sound regime.

In the following section we describe the experimental details. In Sec. III we present our results in the normal fluid and a short sketch of the theory involved in the data analysis. In Secs. IV and V, respectively, the viscosity and the sound velocity of ^{3}He-B is discussed in the framework of recent theories.[13,14] A short conclusion is given in the last paragraph.

II. EXPERIMENTAL

A. Cryostat

A general view of the low-temperature part of the cryostat is shown in Fig. 1. The technique of hyperfine enhanced nuclear cooling of $PrNi_5$ (Ref. 15) was used to cool our ^{3}He sample down to about 1.2 mK. A homemade dilution refrigerator precooled the ex-

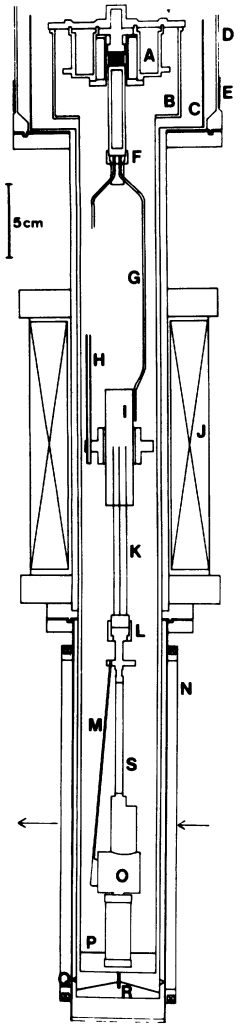

FIG. 1. Schematic drawing of the cryostat. *A*: mixing chamber, *B*: 20-mK radiation shield, *C*: 1-K radiation shield, *D*: vacuum jacket, *E*: compensation coil, *F*: screw contact, *G*: Cu thermal link, *H*: mechanical support of the nuclear stage, *I*: $PrNi_5$ stage, *J*: main magnet, *K*: Cu thermal link, *L*: screw contact, *M*: Ag thermal link, *N*: NMR-split coil (static field in the direction of the arrow), *O*: ^{3}He cell, *P* and *R*: cotton fibers, *Q*: Nylon spacers, and *S*: mechanical support of the ^{3}He cell.

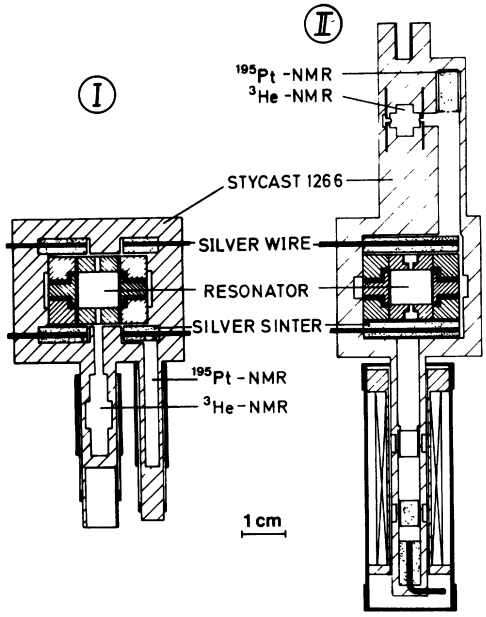

FIG. 2. ^{3}He cells including the coils for NMR on ^{195}Pt and ^{3}He and the cylindrical sound resonators.

perimental cell and the $PrNi_5$ stage (0.25 mol) in a field of 4 T to temperatures of about 15 mK. After decoupling the nuclear stage from the mixing chamber by means of a tin heat switch, we demagnetized usually within about 5 h to a final field of 12.5 mT. This field also kept the Cd solder normal with which the $PrNi_5$ was contacted to the experimental chamber via a thermal link consisting of a bundle of copper wires, a screw joint, a bundle of silver wires, and a silver sinter in the ^{3}He cell. The sinter was made from silver powder (particle size 700 Å), and the resulting surface areas were 18 and 28 m^2, respectively, for the two cells shown in Fig. 2. Both contained a cylindrical sound resonator besides the sinter and two rf coils for pulsed NMR thermometry on ^{195}Pt and ^{3}He. The contamination of our ^{3}He by ^{4}He was less than 15 ppm. (The lower part of cell II shown in Fig. 2 was not used during the experiments described in this paper.) The warm-up rate after demagnetization was typically of the order of 30 μK per hour, which allowed measuring times of more than two days in the superfluid phases of ^{3}He.

B. Pressure determination and regulation

The pressure in the cell was measured by a pressure gauge as described by Straty and Adams.[16] The gauge was situated in the ^{3}He filling capillary. The pressure was determined to an accuracy of 10^{-5} by using a General Radio capacitance bridge (1615 A) and a Ithaco lock-in amplifier (Dynatrac 3) as a zero indicator. This relative accuracy of 10^{-5} was necessary because of the strong pressure dependence of the first-sound velocity, which gives a change in the velocity of about 1000 cm/sec per bar in the range of 8 to 28 bar and which would mask the small tem-

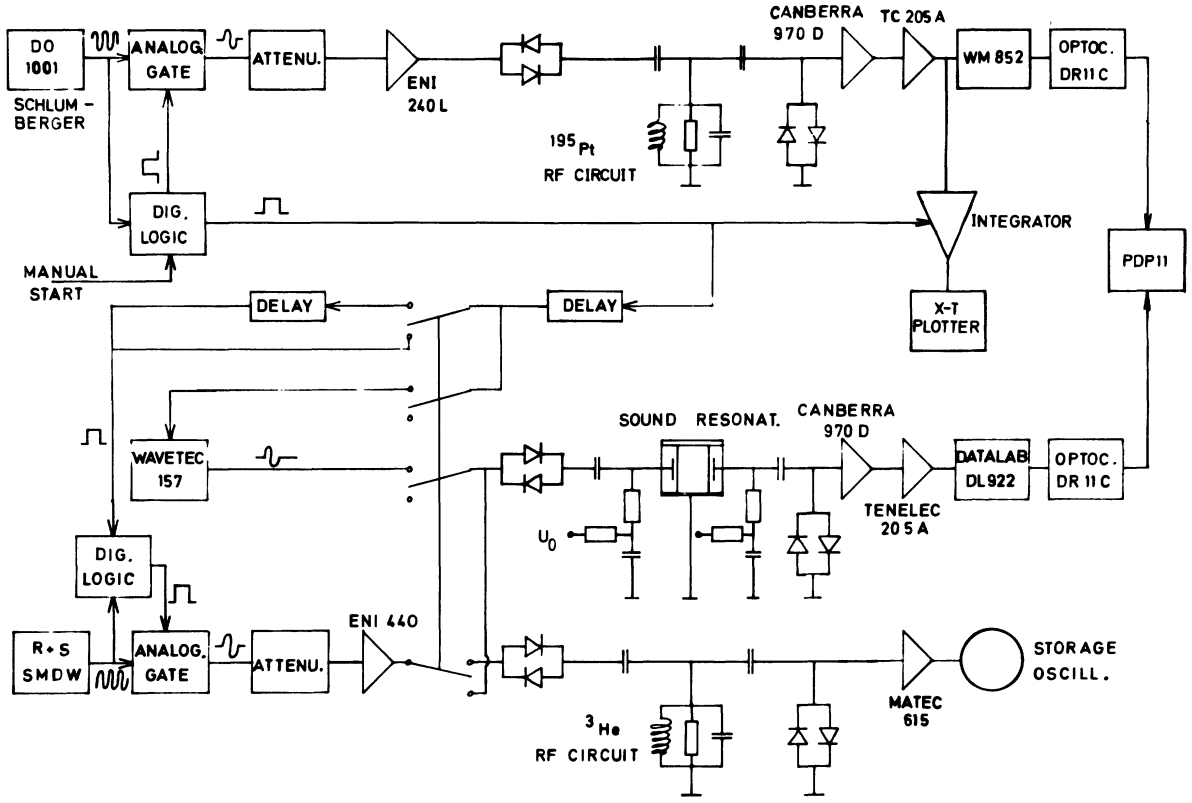

FIG. 3. Block diagram of the pulsed rf spectrometer.

perature dependence of the sound velocity [which is of the order of $(\Delta c_1)/c_1 = 10^{-3}$].

The absolute pressure was determined by a room-temperature manometer (Natec PDCR 10) with a resolution of about 10^{-4}. This meter was also used for the pressure regulation, which was achieved by heating a 1-cm^3 ^{3}He volume weakly coupled to the ^{4}He bath of the cryostat. Thus, the worst pressure shocks (of the order of 10^{-2}) that occurred during the ^{4}He transfers could be regulated within one hour.

C. Pulsed rf electronics

In our experiments the frequency range covered was 20 kHz to 2 MHz, the lower bound applying to the sound experiments and the upper one to NMR on ^{3}He. The pulsed spectrometer that was used is shown in Fig. 3. It consists mainly of commercially available components from which only the feedback capacitor of the Canberra 970D preamplifier was changed to cover the required frequency range. A logic circuit (built in CMOS technique) provided the timing for the pulses and a fixed phase correlation between them by cutting out a preset number of periods from the continuous wave of the frequency synthesizer. The pulse was then attenuated and/or amplified and fed to the NMR coils and/or the sound resonator. There was an odd harmonic distortion of the rf pulse (mainly caused by the analog switch), which, however, was always less than 30 dB.

The NMR coils and the capacitor microphones of the resonator were connected via homemade coaxial lines to the electronics. In the low-temperature part these lines were made from CuNi capillaries and NbTi wires. The impedance of the resonance circuit was never matched to 50 Ω, and the resonance frequency of the NMR coils was usually not tuned to the NMR frequency. The inductance of the rf coils made from 0.05-mm-diam Cu wire was of the order of 300 μH and 1 mH for the He and Pt coils, respectively. The total capacitance of the circuit was of the order of 120 pF and the typical Q values were between 30 and 100. To shorten the ringing-down time of the coil after excitation by the rf pulse, how-

ever, the coils were normally shunted by a metal-film resistor of about 20 kΩ placed at room temperature, yielding Q values of the order of 5.

After an amplification of about 60 dB the response of the rf pulse was monitored either by a storage oscilloscope, an integrator, and a sample-and-hold amplifier or by a transient recorder [20-MHz, 8-bit (binary digit) analog-to-digital converter and 4096 bytes (1 byte=8 bits) of memory]. At a later period of the experiments a Digital Equipment Corporation PDP11/34 computer was available for storage and analysis of the transient spectra. The interface between the computer and the other electronics used had to be made via optocouplers to avoid noise problems. After proper grounding and shielding, signal averaging was not necessary; all data shown in this paper are responses to single pulses.

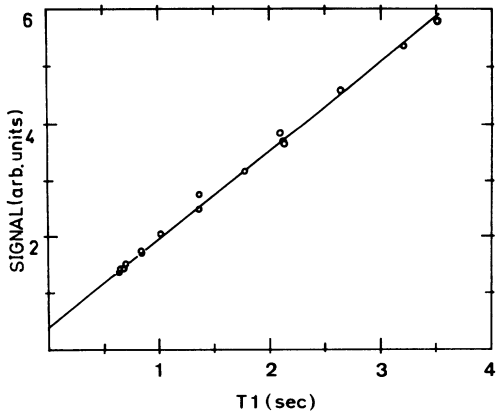

FIG. 4. ^{195}Pt signal after an 8-deg excitation as a function of the spin-lattice relaxation time T_1.

D. Thermometry

The nuclear spin susceptibility of ^{195}Pt was measured by means of pulsed NMR. The static magnetic field H_0 was produced by a rectangularly shaped superconducting split coil, which is shown in Fig. 1. The homogeneity in the center of the coil over 1 cm^3 was better than 100 ppm. However, the main contribution to the inhomogeneity came from the final field of 12.5 mT in the main magnet, which caused a gradient perpendicular to H_0 of 20 μT/cm. The measured decay time of the free induction decay of the Pt was therefore $T_2^* = 1120$ μsec only.

The Pt samples consisting of 10-μm powder (Leico) were directly immersed in the liquid. Two different batches were used in cells I and II. Their weight was 0.8 g and the filling factor about 0.22. The rf field of amplitude $2H_1 = 0.15$ mT was produced by two layers of a cylindrical coil, which was placed outside of cell I but inside of cell II, as shown in Fig. 2. Most of the experiments were done in a static field $H_0 = 26.8$ mT. Thus, irradiating the sample with a pulse of 90 periods of 238-kHz frequency yields a $\pi/2$ excitation of the ^{195}Pt spin system. The $\frac{1}{2}\pi - \Delta t - \frac{1}{2}\pi$ pulse sequence was used to measure the spin-lattice relaxation times T_1. For the susceptibility measurements in most cases an 8° excitation was found to be a good compromise between sensitivity and heating in the temperature range from 1 to 50 mK. At least for sample 2 we ensured that T_2 was temperature independent in the temperature range of interest and found $T_2 = 1880 \pm 100$ μsec by spin-echo measurements, which agrees well with the T_2^* given above.

Normally the Pt was irradiated every 4 min by an 8-deg pulse. The signal was then integrated in the 250 μsec to 1 msec time window either by the amplifer shown in Fig. 3 or by summing over the appropriate channels of the transient recorder with the help of the computer. The thermometer was calibrated in the following way: In the temperature region 10—50 mK a spin-lattice relaxation measurement was compared with the simultaneously measured signal. The result is shown in Fig. 4 from which the extrapolation to $T_1 = 0$ yields the background contribution to the signal. The linear dependence in Fig. 4 indicates that the Korringa law $\kappa = T_1 T = \text{const}$ is obeyed by our sample (actually sample 2). From the signal measured at T_c and the Helsinki temperature scale[17] we can determine $\kappa = 36 \pm 1$ msec K from the slope in Fig. 4. Sample 1 had a Korringa constant $\kappa = 31.95$ msec K.[18] But we would like to mention that due to the uncertainties in κ we never used the absolute value of κ for temperature calibration, we only used the Korringa law to determine the background of the signal that gives a small contribution in the vicinity of T_c.

T_c was detected by the steep drop of the longitudinal relaxation time of the ^{3}He nuclear spin system below the transition temperature.[19] The ^{3}He NMR coil was located near the Pt coil. We believe that we can evaluate the temperature of the Pt powder within a relative accuracy of better than 2%. But due to the heat production in the cell, the complicated flow path of heat within the cell and the finite thermal conductivity of the ^{3}He there was a temperature difference between the thermometer and the sound resonator. To overcome this difficulty we used T_c as indicated by the maximum in the attenuation of first sound at T_c to calibrate the Pt thermometer. Depending on the pulse repetition rate this maximum appeared up to 2 h later than the

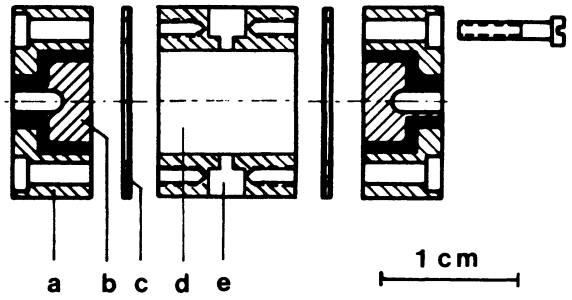

FIG. 5. Sound resonator (cut-away view): *a*, closing disk, *b*, electrode, *c*, aluminized Mylar foil, *d*, ^{3}He sample volume, and *e*, bore for thermal connection to the Ag sinter.

drop in the relaxation time of ^{3}He and had to be determined from an extrapolation in time during the warming up after demagnetization, extrapolated back to T_c from the normal and superfluid sides. Thus, the accuracy of our thermometry is restricted by the availability of first-sound data points near T_c. We feel that the slight discrepancies near T_c between our results (see below Figs. 15–17 and, for example, Refs. 20 and 21) and those of other authors[4–8,22] could be due to remaining temperature gradients in our cells.

E. Sound resonator

The collision time τ of the quasiparticles in ^{3}He increases with decreasing temperature like T^{-2} in the normal fluid and exponentially in the superfluid at the lowest temperatures.[23] To fulfill the hydrodynamic condition $\omega\tau \ll 1$ it was necessary to keep the sound frequency $\nu=\omega/2\pi$ well below 500 kHz. Within our experimental restrictions quartz transducers could not be used. Therefore the sound wave were generated by capacitive transducers as described by Barmatz and Rudnick.[24]

Figure 5 shows a cutaway view of our cylindrical resonator, which was made of copper. The resonator of length $L=1$ cm and of diameter $2R=0.8$ cm was terminated at either end by the two condenser microphones. Their membranes were aluminized Mylar foils of 7 μm thickness, which were stretched and clamped between the copper pieces shown in Fig. 5.

To provide thermal contact between the ^{3}He inside and outside of the resonator the middle piece had two opposite bores of 1 mm diameter. These bores were in the middle of the resonator and are thought to be the origin of the higher damping of the even harmonics of the fundamental plane-wave resonance $\nu_0=c_1/2L$. Therefore only the odd harmonics from the third to the fifteenth, i.e., 40 kHz $<\nu<$ 300 kHz, were measured. Those harmonics were less influenced by the bores than the even harmonics, which have a pressure maximum in the middle of the resonator.

The walls of the resonators were not polished and had a roughness of less than 9 μm with a periodicity of about 50 μm due to machining. The backing electrode of the Mylar foil was isolated from the grounded body of the resonator by Stycast FT. The surface of this electrode was not polished because a roughness of several micrometers is necessary to allow some movement of the foil in its grooves in order to generate the sound wave. The force acting on the foil and correspondingly the sound pressure p is proportional to the square of the applied voltage $U_{\rm eff}$, which is the sum of the bias voltage U_0 and the voltage $U_1\sin(\omega t)$ of the rf pulse, yielding

$$p \propto U_0^2+2U_0U_1\sin(\omega t)+[U_1\sin(\omega t)]^2 . \quad (1)$$

From Eq. (1) it is obvious that U_0 should be as high as possible for large signals and negligible nonlinear contributions. We used $U_0=400$ V and an ac voltage U_1 of about 1 V. Thus, in addition to the distortion factor of the electronics, only pressure oscillations of frequency ω were excited and observed.

Our pulsed method of measuring the first sound attenuation and velocity was as follows: Before the application of a rf pulse the pressure in the cell was monitored as described above and the temperature was measured with the ^{195}Pt NMR system. After a delay time of 20 msec, which was short compared to the thermal equilibration times within the cell, the resonator was automatically excited by the application of 500 to 1000 periods of the desired frequency ω on one foil. During this time (typically 5 msec) a standing sound wave was generated and had reached a constant amplitude. With the end of the last period of the rf pulse the transient recorder was triggered and the free decay of the standing wave was monitored. Figure 6 shows the result of such a measurement. The wave was detected either by the same foil or by the opposite receiver foil. Both techniques were used and gave identical results for the attenuation, indicating that the influence of the foils themselves and their backing is of no significance.

The exponential decay shown in Fig. 6 is proportional to $\exp(-\alpha c_1 t)$, where the sound velocity c_1 is given by

$$c_1=\frac{\omega L}{\pi n} , \quad (2)$$

and n is the order of the harmonic. In Fig. 6 it is also seen that the decay takes place in steps, which is a direct consequence of the time-of-flight character of our measurement where each pulse train of n

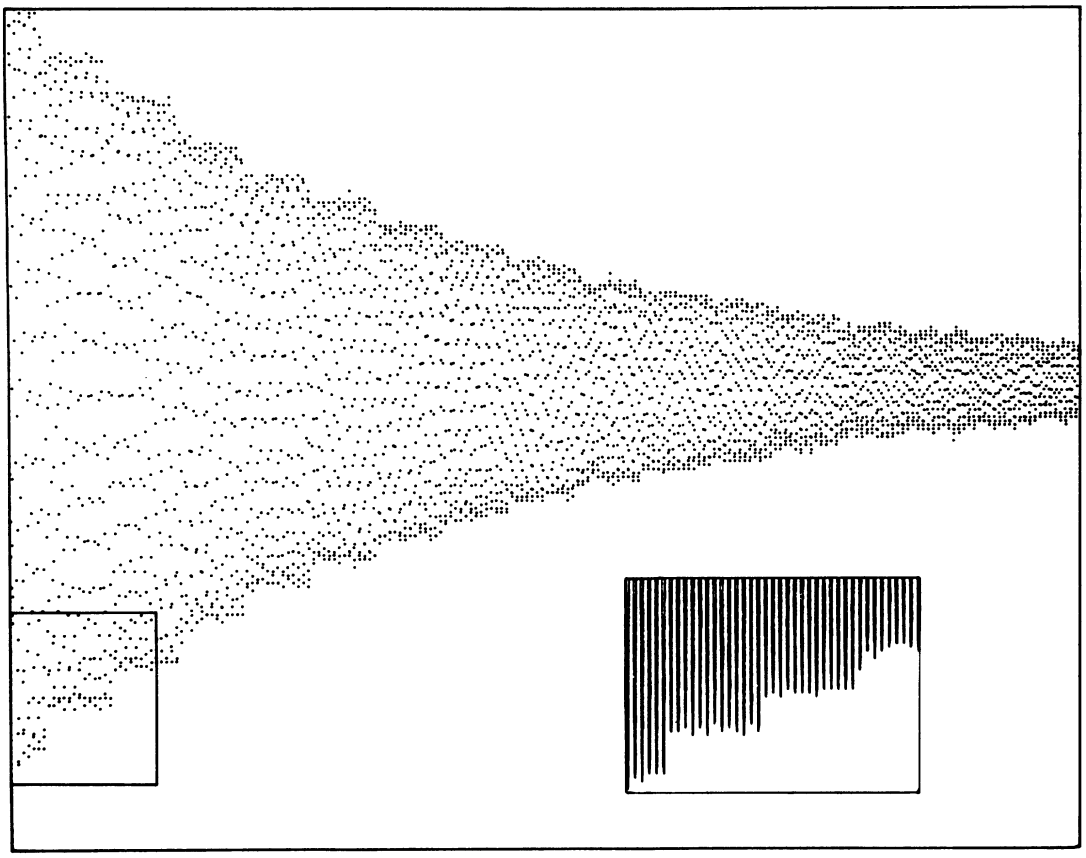

FIG. 6. Free decay of the sound wave shown is the 13th harmonic obtained at 28 bar and a temperature of about $0.9T_c$. Total length of the trace is 0.8 msec. Inset shows the beginning of the decay on doubled time scale. Step structure of the exponential decay is a consequence of the reflection of the wave train (13 periods) at the membranes.

periods has the same history between two reflections on the same foil. The inset in Fig. 6 shows the beginning of the decay on an enlarged time scale. From this one can see that the thirteenth harmonic was measured with the receiver foil. This step structure is stronger with higher attenuation, and the sharpness of the steps reflects directly the quality of the resonator concerning the plane parallelism and homogeneity of the foils: the sharper the better. (We had several difficulties with the foils ranging from cracks on the corners after heavy use up to dissolution of the aluminized layer due to some reaction with the copper body in the presence of humidity during test measurements. Such difficulties always led to a smearing out of the step structure.)

There is no beat of neighboring frequencies visible in Fig. 6 indicating that there are no contributions from radial or mixed radial-axial modes to the signal even at higher harmonics where the abundance of those modes increases.[25] In cw experiments nonaxial modes could be excited up to 20% of the amplitude of the pure axial modes. But in an rf pulse of 500 periods the frequency bandwidth is smaller than the frequency difference between the harmonics under consideration and between all other modes. In Fig. 7 the Fourier transform of the transient

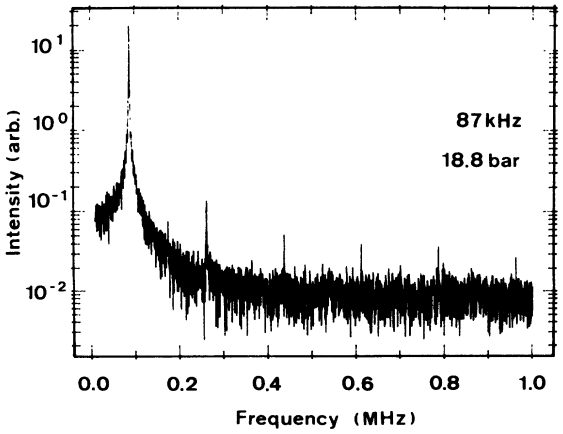

FIG. 7. Fourier spectrum of the 5th harmonic.

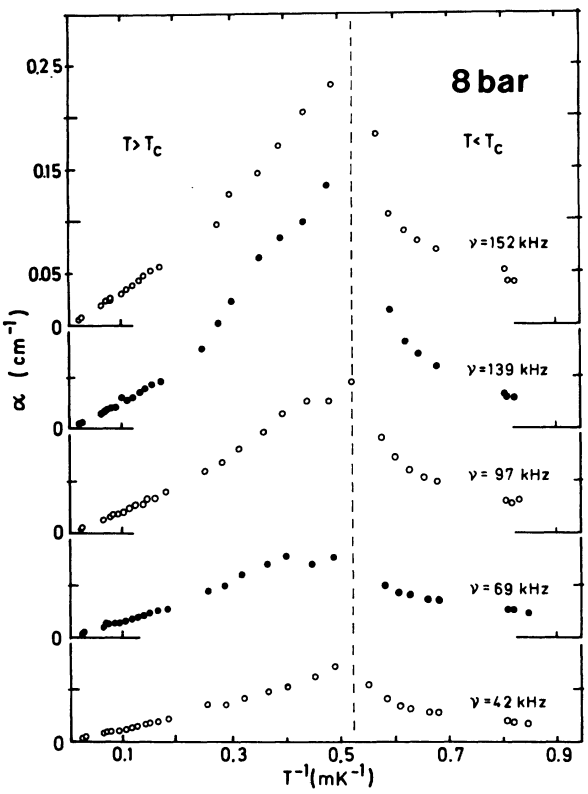

FIG. 8. Attenuation of first sound vs the inverse temperature in cell 1 at 8 bar. Background attenuation is subtracted.

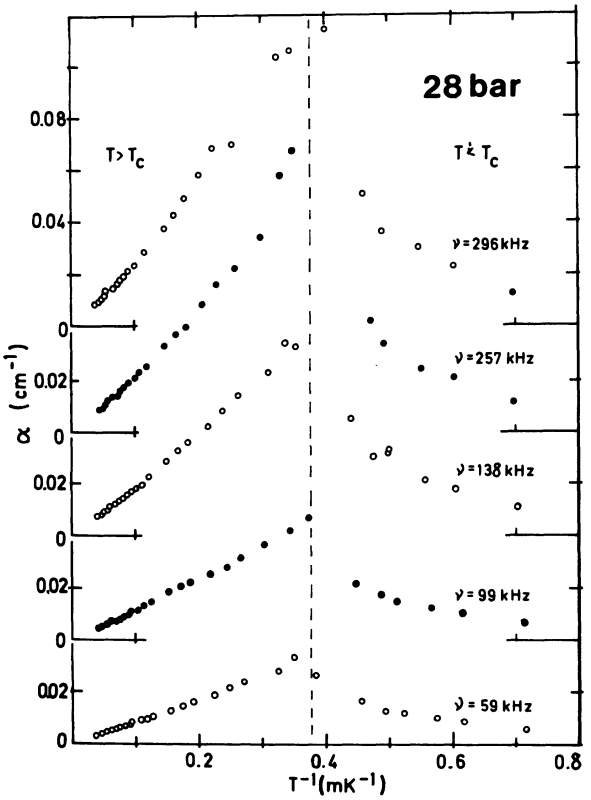

FIG. 9. Attenuation of first sound vs the inverse temperature in cell 1 at 28 bar. Background attenuation is subtracted.

spectrum of the fifth harmonic is shown. Besides the odd harmonics due to the distortion factor of the electronics no other resonances except the fifth can be detected.

In principle, all these resonances should be considered if the data were analyzed by fitting the function

$$f(t)=A\exp(-\alpha_{\rm exp}c_1 t)\sin(\omega t+\varphi) \qquad (3)$$

to a transient spectrum like Fig. 6. But within our accuracy no deviations in $\alpha_{\rm exp}$ and c_1 could be found by fitting the irradiated harmonic only (the steps do not influence $\alpha_{\rm exp}$ and c_1). Therefore, analyzing our data we used Eqs. (2) and (3) for one frequency only to obtain the velocity of first sound c_1 and the damping $\alpha_{\rm exp}$ of the resonator, respectively. Evidently, to determine the attenuation of first sound α some background damping α_0 must be subtracted from $\alpha_{\rm exp}$. The background damping corresponds to quality factors of the order of 1000 and can be measured in principle at high temperatures ($T>300$ mK) where the damping due to the low viscosity of the liquid is negligible. It turns out that α_0 does not depend on the temperature, but only depends on the frequency. We believe that most of the background damping is caused by interaction with the membranes. Thus we evaluate α according to Eq. (4),

$$\alpha(\omega,T)=\alpha_{\rm exp}(\omega,T)-\alpha_0(\omega)\ , \qquad (4)$$

where $\alpha_0(\omega)=\alpha_{\rm exp}(\omega,T\to\infty)$.

III. THEORY AND NORMAL-FLUID RESULTS

The measured transient spectra were analyzed according to Eqs. (2)—(4) yielding the velocity and the attenuation of first sound. Figures 8—13 show the results in normal and superfluid ^{3}He as a function of the inverse temperature. For all pressures and frequencies the sound velocity (Figs. 12 and 13) drops in the normal fluid with decreasing temperature and grows again in the superfluid whereas the attenuation (Figs. 8—11) behaves in just the opposite way. Before discussing the superfluid data we would like

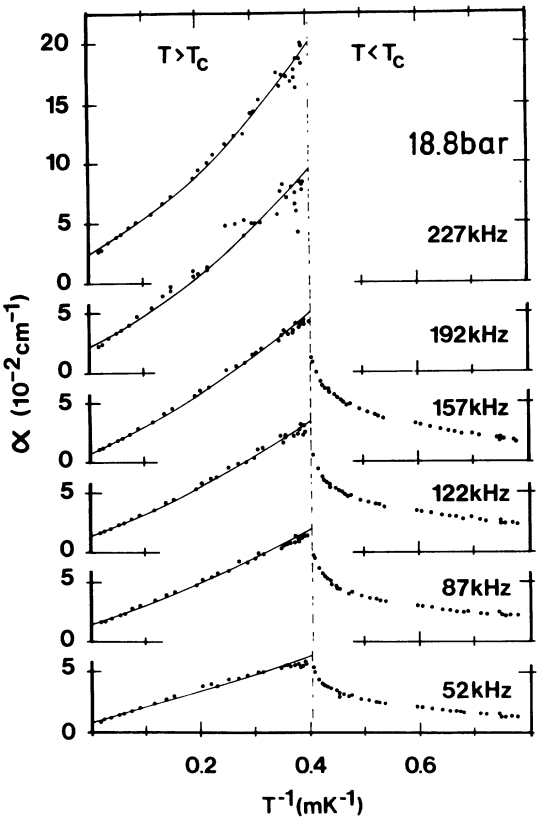

FIG. 10. Attenuation of first sound vs the inverse temperature in cell 2 at 18.8 bar. Curves are calculated with the use of the viscoelastic model (Ref. 13) and assuming a temperature-independent background attenuation.

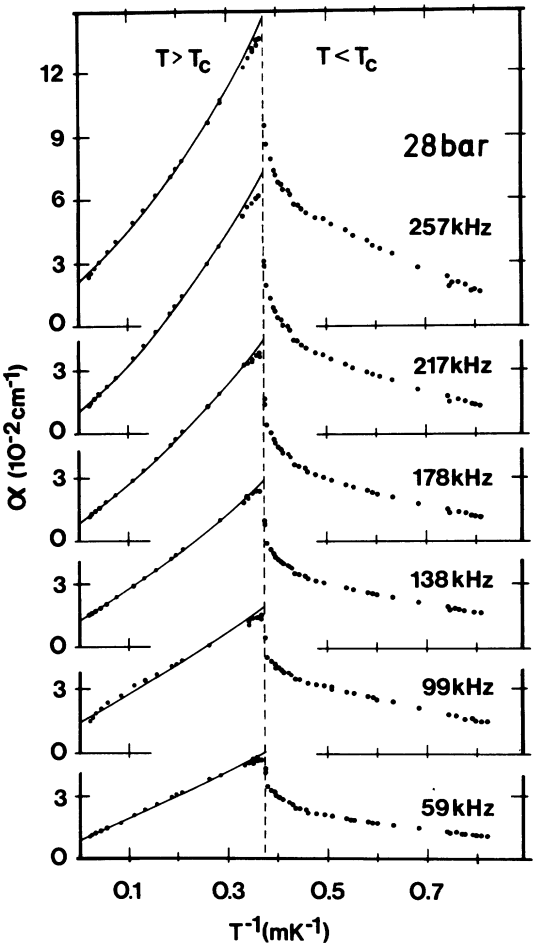

FIG. 11. Attenuation of first sound vs the inverse temperature in cell 2 at 28 bar. Otherwise same as in Fig. 10.

to present the theory and analyze the results obtained in the normal fluid.

A. Attenuation

In the hydrodynamic limit $\omega\tau \ll 1$ with τ being the quasiparticle collision time the attenuation is given by[26]

$$\alpha = \frac{2\eta\omega^2}{3\rho c_1^3} + \frac{\omega\delta}{2Rc_1} , \tag{5}$$

with η being the viscosity and ρ the density of the liquid. R is the radius of the resonator and δ the viscous penetration depth

$$\delta = \left[\frac{2\eta}{\rho\omega}\right]^{1/2} . \tag{6}$$

The first term of Eq. (5) is a contribution due to the scattering of the quasiparticles on each other and varies in the normal fluid with T^{-2} because $\eta T^2 = \text{const.}$[27] In our geometry this bulk contribution α_b to the damping is dominated by the second term of Eq. (5) which describes the scattering of the quasiparticles on the walls. This term (α_w) increases like T^{-1}. The stronger influence of the bulk attenuation at lower temperatures and higher frequencies is clearly demonstrated by Fig. 9 where (as well as in Fig. 8) a frequency-dependent background attenuation α_0 was subtracted according to Eq. (4). The assumption of the temperature independence of α_0 appears justified by the agreement between the data of Figs. 10 and 11 and the theory of Nagai and Wölfle[13] (see below).

In this theory a viscoelastic model description of ^{3}He is employed which works in the hydrodynamic as well as the collisionless regime. The attenuation is then expressed by

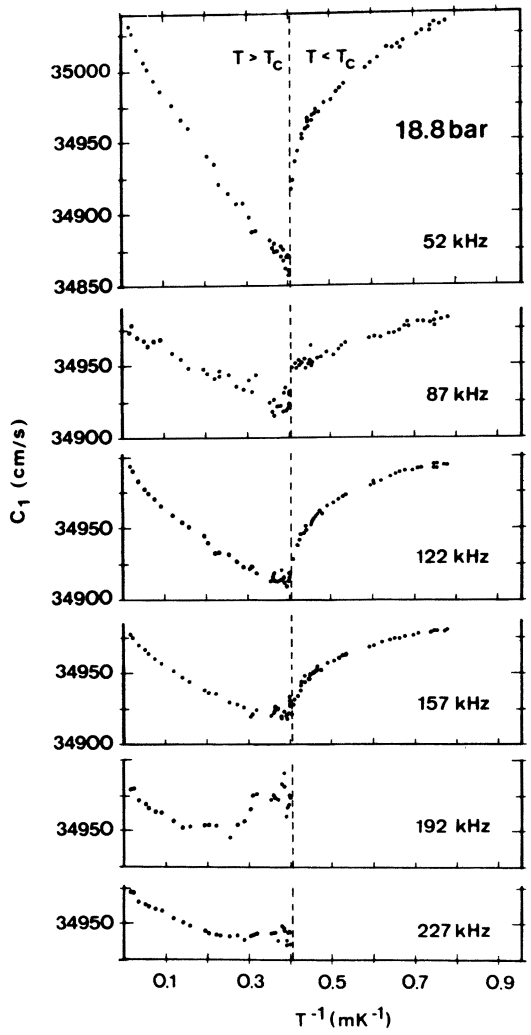

FIG. 12. First-sound velocity at 18.8 bar vs the inverse temperature.

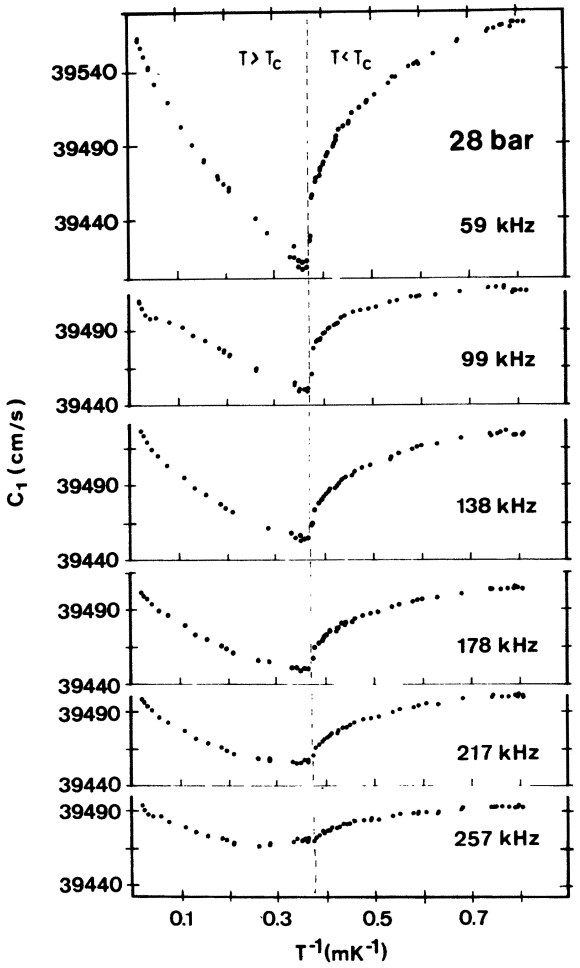

FIG. 13. First-sound velocity at 28.0 bar vs the inverse temperature.

$$\alpha=\frac{2\omega^2}{3\rho c_1^3}\mathrm{Re}\left[\frac{\eta}{1-i\omega\tau_\eta}\right]+\frac{1}{\rho R c_1}\mathrm{Re}[Z(\omega)]\ . \tag{7}$$

The first and second terms being again α_b and α_w. But now the wall attenuation is described by the real part of the complex surface impedance $Z(\omega)$ and the bulk attenuation is modified by the viscous relaxation time τ_η which may be related to the quasiparticle collision time τ and the viscosity η according to

$$\tau_\eta=\frac{\tau}{1-\lambda_2\dfrac{Y_2}{Y_0}} \tag{8}$$

and

$$\eta=\tfrac{1}{5}\rho\frac{m^*}{m}Y_0\langle v^2\rangle\tau_\eta\ . \tag{9}$$

We introduced here the generalized Yoshida functions Y_i (with $Y_i=1$ in the normal fluid) as defined in Ref. 10. The other parameters have their usual meaning and were taken from Ref. 27. The mean value of the quasiparticle velocity $\langle v^2\rangle$ is related to the Fermi velocity by

$$\langle v^2\rangle=v_F^2\frac{Y_2}{Y_0}\ . \tag{10}$$

In the surface impedance $Z(\omega)$ mean-free-path effects are included especially the slip effect. A slip of the fluid velocity at a wall occurs when the mean free path $\lambda=v_F\tau$ of the quasiparticles becomes com-

parable to the viscous penetration depth δ. According to the work of Jensen *et al.*[14] the slip can be characterized by the complex slip length

$$\xi=\frac{8\eta_t(\omega)\left[1-ik_3v_F\tau\left[\frac{8}{15}\frac{Y_2}{Y_1}-\frac{3}{8}\frac{Y_1}{Y_0}\right]\right]}{3\rho\frac{m^*}{m}v_F Y_1(1-i\omega\tau)}, \tag{11}$$

where

$$\eta_t(\omega)=\frac{\eta}{1-i\omega\tau_t}. \tag{12}$$

The wave vector k_3 of the transversal waves is given by

$$k_3=\left[i\frac{\omega\rho_n}{\eta_t(\omega)}\right]^{1/2}, \tag{13}$$

and the normal-fluid density ρ_n is usually expressed by

$$\frac{\rho_n}{\rho}=\frac{[1+(F_1/3)]Y_0}{1+(F_1/3)Y_0}. \tag{14}$$

Following Nagai and Wölfle[13] the surface impedance can then be expressed by

$$Z(\omega)=\frac{[-i\omega\rho_n\eta_t(\omega)]^{1/2}}{1-i\xi k_3}, \tag{15}$$

which may be expanded for $\omega\tau\ll 1$ yielding

$$Z(\omega)=\omega\rho_n[(1/k_3)+i\xi]. \tag{16}$$

Thus, in the hydrodynamic regime one gets

$$k_3=\frac{1+i}{\delta} \tag{17}$$

and

$$\xi=\tfrac{8}{15}\lambda\left[1+\frac{19}{120}\frac{\lambda}{\delta}(1-i)\right], \tag{18}$$

from which it is obvious that the effect of slip on the attenuation is much smaller than on the velocity of sound because $\frac{19}{120}(\lambda/\delta)\ll 1$.

But there are still corrections from the more detailed theory of the sound attenuation in a cylindrical resonator[28] yielding an additional term in the damping of the sound waves

$$\alpha_{\text{add}}=\frac{\omega^2}{4\rho c_1^3}\text{Re}[X(\omega)], \tag{19}$$

where

$$X(\omega)=\eta_t(\omega)\left[1-\frac{8L}{(\pi n)^2R}+2\left[\frac{L}{\pi nR}\right]^2\right], \tag{20}$$

and n is the number of the harmonic under consideration. The additive attenuation according to Eq. (19) has the same η and ω dependency as the bulk contribution in Eq. (5).

The curves shown in Figs. 10 and 11 are the best fits of Eqs. (4), (7), and (19) to our measurements with ηT^2 and α_0 as free parameters. Slight systematic deviations from this theory are visible. Especially near T_c the attenuation is about 3% lower than expected. A similar behavior was found in the torsional oscillator experiment by Parpia *et al.*[5] and very recently in a vibrating-wire experiment by Carless *et al.*[29] It has been suggested[5] that these deviations may be caused by fluctuation effects near T_c. But fluctuation effects are expected only much closer to T_c. At present a satisfactory explanation of this behavior is still missing.

In Table I (first line) the mean values of ηT^2 obtained in both experimental cells are compiled. The errors given in Table I are the weighted deviations of the mean of each harmonic. The larger errors of the results of cell 2 which should be of more statistical significance compared with those of cell 1 indicate that there are still some systematic errors. Most of them may be connected with the observation of an increase by about 20% in ηT^2 down to the lowest frequency as well as the fact that the sound velocity c_1 extrapolated for $T\to\infty$ increases also by about 0.2% (see below). At present we have no explanation for this behavior. But still the values given in Table I agree well with the pressure dependence observed by other authors.[30,31,27]

TABLE I. Pressure dependence of ηT^2.

	Cell 1		Cell 2	
Method	8 bar	28 bar	18.8 bar	28 bar
Attenuation	1.59(9)	1.11(9)	1.53(18)	1.26(10)
Velocity			1.38(30)	1.23(20)

B. First-sound velocity

The sound velocity is given in the viscoelastic theory by

$$c_1 = c_\infty \left[1 + \mathrm{Im} \left[\frac{2\omega\eta}{3\rho c_\infty^2 (1 - i\omega\tau_\eta)} + \frac{1}{\omega\rho R} Z(\omega) + \frac{\omega}{4\rho c_\infty} \frac{\rho_n}{\rho} X(\omega) \right] \right] . \quad (21)$$

c_∞ is the first-sound velocity at high temperatures ($\eta \to 0$) which should be equal to the velocity of the infinite bulk liquid ($R \to \infty$). The second term in Eq. (21) arises from zero-sound contributions and the third and fourth term take into account the influence of the resonator wall. In the hydrodynamic regime and neglecting the slip effect Eq. (21) reduces to the well-known formula

$$c_1 = c_\infty [1 - (\delta/2R)] . \quad (22)$$

Owing to the slip effect,

$$\Delta c_s = c_\infty \frac{8}{15} \frac{\lambda}{R} \quad (23)$$

must be added which is of opposite sign to the wall contribution in Eq. (22). For higher frequencies contributions of zero sound must be taken into account even in the normal fluid which adds

$$c_z = \frac{\eta\omega^2\tau_\eta}{\rho c_\infty [1 + (\omega\tau_\eta)^2]} \left(\tfrac{2}{3} + \tfrac{1}{4}\right) . \quad (24)$$

The second term in Eq. (24) again arises from the boundary conditions according to Ref. 28.

In Fig. 14 we compare the theory [Eqs. (21), (23), and (24)] with our measurement at pressures of 18.8 and 28 bar and for the highest frequencies applied. The influence of the slip effect is clearly demonstrated as well as zero-sound contributions by shifting from the dashed line (hydrodynamic limit) via the dashed-dotted line which includes the slip effect to the solid line which is the description according to the full theory. Thus, below about 5 mK, zero-sound corrections must be taken into account. But the main deviation from the hydrodynamic behavior is caused by the slip effect.

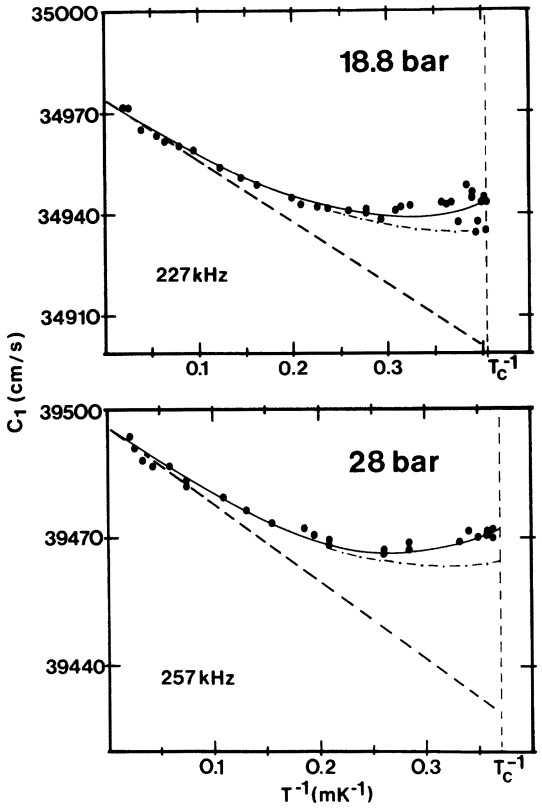

FIG. 14. First-sound velocity in the normal fluid. Curves give the hydrodynamic limit (dashed line), the slip correction (dashed-dotted line), and the full theory including zero-sound corrections (solid line).

Fitting our data (Figs. 12 and 13) by only two free parameters ηT^2 and c_∞ according to Eq. (21) we obtain the values given in Tables I and II. It can be seen that the attenuation and the velocity measurement give the same value for ηT^2 within the experi-

TABLE II. First-sound velocity c_1 of the bulk liquid and the deviation of the nth harmonic from the velocity measured for the 11th harmonic (values given in cm/sec for $T \to \infty$).

	c_1		$\Delta c_1 = c_1(n\text{th}) - c_1(11\text{th})$ Harmonic number			
	Ref. 27	This work	3	7	9	13
18.8 bar	34913.	34974.5(0.5)	62.5(3.4)	11.8(2.0)	0.6(1.0)	−0.5(0.5)
28.0 bar	39387.	39495.5(0.5)	69.3(2.6)	25.7(2.0)	3.5(1.0)	0.5(0.5)

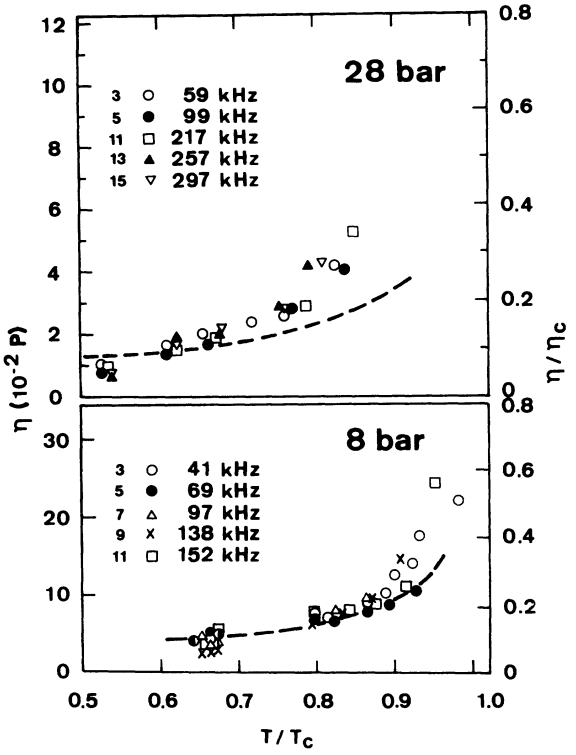

FIG. 15. Shear viscosity (in poise) in ^{3}He-B for 28 and 8 bar vs the reduced temperature as obtained with cell 1. Results for different resonance frequencies are shown which are correlated to the number of the harmonics given in front of the signs. Also shown by the dashed lines are the smoothed results of Ref. 6.

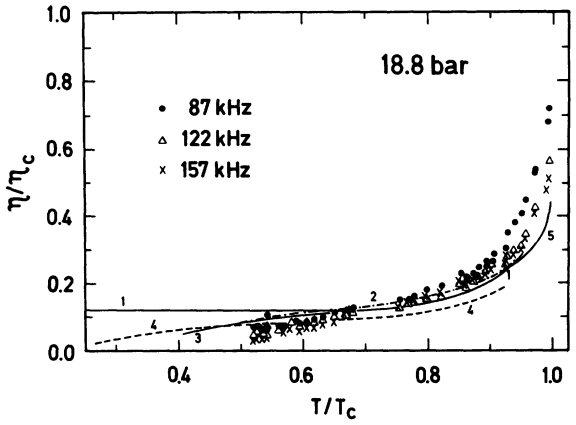

FIG. 16. Shear viscosity in ^{3}He-B for 18.8 bar vs the reduced temperature as obtained with cell 2. Definition of the characters is the same as for Fig. 15. Also shown are the theoretical results of Ref. 32 by curve 1 and experimental results of Refs. 7, 7, 8, and 22 by the curves 2, 3, 4, and 5, respectively.

mental error indicating no larger additive contributions to the attenuation, e.g., from some ^{3}He in the grooves of the backing electrodes. In the second column of Table II the sound velocities are compared with those of Ref. 27 which agree very well with our values given in the third column. These values are the result for the 11th harmonic and are similar for all higher harmonics. The deviations of the sound velocity determined for the nth harmonic from that of the 11th are also given in Table II. The increase in the velocity with lower frequencies is not understood yet. But we feel that the viscoelastic theory yields an adequate description of our results in the normal fluid encouraging us to apply it to our data obtained in the superfluid phase.

IV. VISCOSITY OF SUPERFLUID ^{3}He

In contrast to the normal fluid where the temperature dependence of η is known to be $\eta T^2 = \text{const}$ the viscosity of the superfluid must be determined from the zeros of the combined Eqs. (4), (7), and (19) which we obtained by an iterative method. For the normal-fluid density the theoretical value was taken according to Eq. (14) with the use of the Landau and gap parameters as well as the jump in the specific heat given in the work of Alvesalo *et al.*[17] We have not taken into account the older values[27] which would only slightly affect the reduced viscosity as shown by Ono *et al.*[32] We made sure that only one root for η existed in the region covered by the data. The results are presented in the Figs. 15–17 and confirm again the observa-

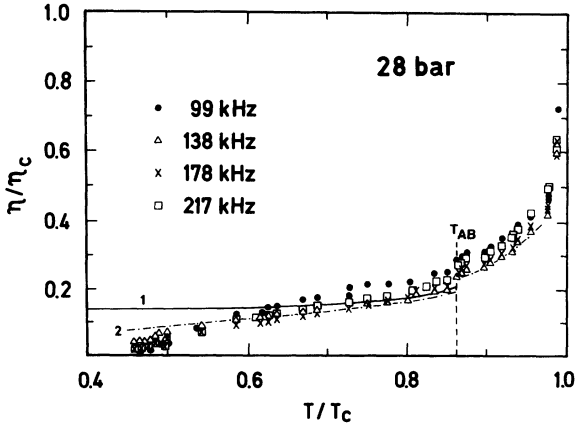

FIG. 17. Shear viscosity in ^{3}He-B for 28 bar vs the reduced temperature as obtained with cell 2. Curves 1 and 2 are according to Refs. 32 and 7, respectively.

tion of a steep drop of the viscosity just below the transition temperature with a subsequent continuous decrease down to the lowest temperatures. In each figure η/η_c is calculated with the use of the temperature scale established by the method described in Sec. II D. The measurements in cell 1 shown in Fig. 15 which we reported earlier[20] have larger uncertainties in the temperature scale as discussed briefly in Sec. II and in more detail elsewhere.[33] We believe that the discrepancy near T_c between our results and those of Archie *et al.*[7] which are also shown by the dashed lines in Fig. 15 could be removed if we knew more precisely the transition temperature in the sound resonator as we do for the measurements in cell 2 which are presented in Figs. 16 and 17.

But even there a systematic tendency remains so that our results for the reduced viscosity close to T_c are slightly higher than those of other authors as shown in the figures by the different curves. As most of all other investigations on the viscosity were done either in geometries providing a better heat flow or using lanthanum-diluted cerium magnesium nitrate thermometry with less heat production we must assume that even 0.3 nW which was the average heat leak due to the NMR pulses was still enough in our experiment to produce a $\Delta T/T$ of the order of 3% between the Pt powder and the sound resonator. Such a gradient would be sufficient to explain the deviation near T_c from the results of other authors. This temperature gradient should be smaller at lower temperatures because the thermal conductivity of the ^{3}He increases with the increase of the superfluid density ρ_s.

Lowering the heat production within our Pt sample with the use of smaller tipping angles would reduce the thermal gradients but would also increase the error in the temperature determination due to larger uncertainties in the NMR signal. Thus, because of experimental difficulties and the lack of knowledge of the detailed heat flow within our cell we can only estimate the error in the temperature of the sound resonator to be of the order of 5%.

The data of the 18.8- and 28-bar experiments displayed in Figs. 16 and 17, respectively, do not include the third harmonic which gave incorrect results for ηT^2 in the normal fluid. This observation was not made in the experiments with cell 1. Therefore we believe that the deviations are associated with the holes in the center of the resonator wall. It is likely that a larger fraction of the fluid is flowing through the holes at lower frequencies. The 11th (192 kHz) and 13th (227 kHz) were not measured in case of 18.8 bar. At 28 bar the 13th (257 kHz) is omitted because at our lowest temperatures we observed a smaller sound attenuation than expected from the quality factor of the resonator at this frequency. Whether this is due to an experimental fault or due to the invalidity of the assumption of a temperature-independent background attenuation could not be clarified. Beside this no further frequency dependence could be detected.

Thus, by and large, all experiments are in accordance and as far as the pressure and temperature dependence is concerned they can be explained very well by the *s-p-d* approximation of Ono *et al.*[32] which is also shown as a solid line in the Figs. 16 and 17. This is, however, only true for $T>0.6T_c$. For lower temperatures the theory no longer describes the experiments which still show a decrease of the viscosity with decreasing temperature whereas the theory predicts a shallow minimum in η around $T=0.6T_c$. The fact that η still decreases at the lowest temperatures measured could mean that there is more structure in the scattering amplitude of the quasiparticles. This is an open question and remains subject to further investigations.

At the transition between the *B* and *A* phases there is a step in our viscosity data similar to that observed by Archie *et al.*[7] But even in our simple geometry where the wave vector of the sound was parallel to the magnetic field which was aligned in the direction of the axis of the resonator it is not clear which parts of the viscosity tensor are really probed. As a first step we neglected this and analyzed the attenuation in the *A* phase in the same way as in the *B* phase. But, to have interpretable results for the anisotropy of η more sophisticated experimental arrangements seem to be necessary as well as a more detailed analysis to separate—if possible—the different components of the viscosity tensor.

V. SOUND VELOCITY OF SUPERFLUID ^{3}He-*B*

In the superfluid Eq. (22) has to be modified by

$$c_1=c_\infty\left[1-\frac{\delta_s}{2R}\frac{\rho_n}{\rho}\right], \tag{25}$$

where $\delta_s=(2\eta/\omega\rho_n)^{1/2}$. From Eq. (25) the observed temperature behavior (see Figs. 12 and 13) is qualitatively clear: The sound velocity has to rise again in the superfluid to its high-temperature value because the viscosity becomes small and the normal-fluid density vanishes for $T\to 0$. If, however, we calculate quantitatively c_1 from Eq. (21) with the use of our results for the viscosity as presented in the foregoing section we obtain the curve shown in Fig. 18. Obviously it deviates significantly from the measured velocity especially at lower temperatures.

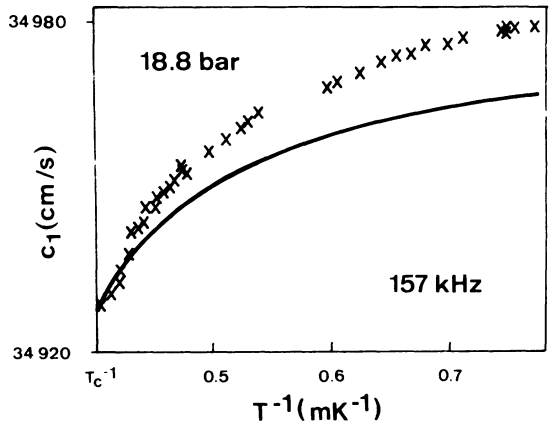

FIG. 18. First-sound velocity in ^{3}He-B vs inverse temperature. Experiment was performed at 18.8 bar and 157 kHz. It is compared with the theoretical velocity obtained from the viscosity shown in Fig. 16 according to Ref. 13 assuming purely diffuse scattering.

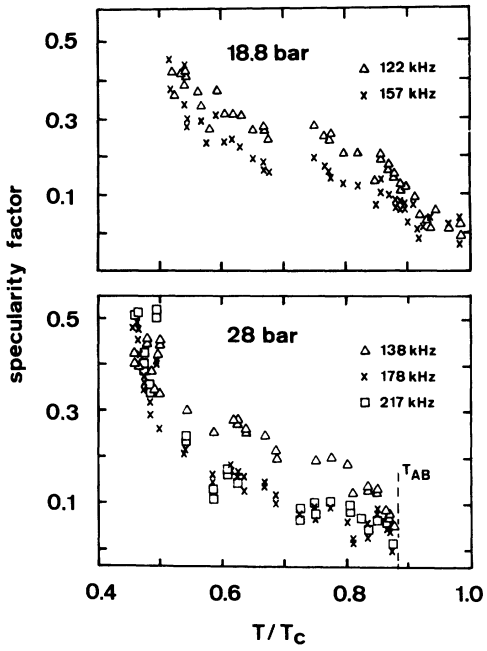

FIG. 19. Specular-reflection factor vs the reduced temperature as obtained by a consistency argument for the results from the sound-absorption and velocity measurement. This factor would remove the discrepancy in Fig. 18.

This discrepancy (briefly reported in Ref. 34) is found for all pressures and frequencies used and cannot be due to the uncertainties in the Landau or gap parameter, in the jump of the specific heat or in ρ_n/ρ. For example, ρ_n/ρ should be only half of its accepted value at $T=0.5T_c$ to remove the deviation. We also rule out thermal gradients as a possible cause for this discrepancy because in that case it should decrease as the temperature is lowered owing to the increasing thermal conductivity of the liquid.

One possibility to explain this behavior would be to modify the slip length ξ given in Eq. (11) due to the fact that not only diffuse scattering but also specular reflection of the quasiparticles at the walls takes place. Specular reflection leads to an enlarged slip length which in turn increases the sound velocity. If we allow for partly specular reflection which means replacing ξ by $\xi=\xi(1+s)/(1-s)$ where s is the specularity factor[14] (equal to 1 or 0 for specular reflection or diffuse scattering, respectively) we can calculate s on the condition that the theoretical curve of Fig. 18 must coincide with the experimental data. The result for s is given in Fig. 19 which shows a continuous increase of the specularity factor with decreasing temperature. At $T=0.5T_c$ almost 40% of the quasiparticles would be specularly reflected. A finite value for s would slightly change our results for the viscosity, but at present we prefer not to modify our results because there is no theoretical description of the reflection process.

We may, however, speculate[35] whether our result of an increasing specularity factor could be related to the following observation made with negative ions in superfluid ^{3}He. The steep increase of the ion mobility below T_c was explained[36] by a temperature-dependent differential scattering cross section which peaks increasingly in the forward direction as the temperature is lowered.[37] This effect is insensitive to the size of the scattering center. Now, there is a certain similarity between forward scattering and specular reflection, in the sense that the parallel momentum is conserved. If this analog is correct, it seems plausible that s increases as the temperature is reduced. Even if this speculation is wrong, it might well be that the reflection of a quasiparticle at a wall is influenced by pairing and there is little reason to assume that s vanishes identically at all T/T_c. We expect that this effect is not caused by the microscopic smoothness of the surface but rather by a quantum-mechanical interference effect associated with the pair correlations. It is desirable to have a theoretical investigation of this problem.

VI. SUMMARY AND CONCLUSION

We have shown that measurements of the velocity of first sound in a cylindrical resonator can be per-

formed with high resolution. Thus, we could clearly separate mean-free-path effects and zero-sound contributions. The slight increase of the velocity in the normal fluid with decreasing frequencies remains unclear. In the superfluid we can explain our data only by assuming partly specular reflection instead of purely diffuse scattering at the walls of the container.

For the viscosity of ^{3}He-B we obtain the same continuous decrease with decreasing temperature as observed in earlier experiments which were done using torsional oscillators or vibrating wires. Therefore we must conclude that the deviations from the theory at temperatures below $0.6T_c$ are serious. An explanation for this effect is missing. Thus, further theoretical and experimental progress in both the normal-fluid and the superfluid phase of ^{3}He is necessary.

ACKNOWLEDGMENTS

It is a pleasure to acknowledge the theoretical support by Professor P. Wölfle, which was supplied with great patience. We would also like to thank Dr. D. Einzel, Dr. E. Hagn, and Dr. E. Zech for many fruitful discussions. The experimental help of B. Amend, H. Angerer, H. Hagn, and H.-G. Willers is gratefully acknowledged. This work was supported by the Deutsche Forschungsgemeinschaft.

---

*Permanent address: Fakultät für Physik, Universität Regensburg, D-8400 Regensburg, Federal Republic of Germany.

[1]D. D. Osheroff, R. C. Richardson, and D. M. Lee, Phys. Rev. Lett. 28, 885 (1972).

[2]T. A. Alvesalo, H. K. Collan, M. T. Loponen, O. V. Lounasmaa, and M. C. Veuro, J. Low Temp. Phys. 19, 1 (1975).

[3]T. A. Alvesalo, C. N. Archie, A. J. Albrecht, J. D. Reppy, and R. C. Richardson, J. Phys. (Paris) Colloq. 39, C6-41 (1978).

[4]P. C. Main, C. W. Kiewiet, W. T. Band, J. R. Hook, D. J. Sandiford, and H. E. Hall, J. Phys. C 9, L397 (1976).

[5]J. M. Parpia, D. J. Sandiford, J. E. Berthold, and J. D. Reppy, Phys. Rev. Lett. 40, 565 (1978).

[6]C. N. Archie, T. A. Alvesalo, J. D. Reppy, J. E. Berthold, and R. C. Richardson, J. Phys. (Paris) Colloq. 39, C6-37 (1978).

[7]C. N. Archie, T. A. Alvesalo, J. D. Reppy, and R. C. Richardson, J. Low Temp. Phys. 42, 295 (1981).

[8]D. C. Carless, P. W. Alexander, H. E. Hall, J. R. Hook, and N. V. Wellard, Physica 108B, 793 (1981).

[9]C. J. Pethick, H. Smith, and P. Bhattacharyya, Phys. Rev. B 15, 3384 (1977).

[10]P. Wölfle and D. Einzel, J. Low Temp. Phys. 32, 38 (1978).

[11]M. Dörfle, H. Brand, and R. Graham, J. Phys. C 13, 3337 (1980).

[12]J. Hara and Y. A. Ono, Phys. Lett. 81A, 65 (1981); Y. A. Ono and J. Hara, J. Phys. C 14, 2093 (1981).

[13]K. Nagai and P. Wölfle, J. Low Temp. Phys. 42, 227 (1981).

[14]H. H. Jensen, H. Smith, P. Wölfle, K. Nagai, and T. Maack Bisgaard, J. Low Temp. Phys. 41, 473 (1980).

[15]K. Andres and S. Darack, Physica 86-88B + C, 1071 (1977).

[16]G. C. Straty and E. D. Adams, Rev. Sci. Instrum. 40, 1393 (1969).

[17]T. A. Alvesalo, T. Haavasoja, and M. T. Manninen, J. Low Temp. Phys. 45, 373 (1981).

[18]D. D. Osheroff (private communication).

[19]L. R. Corruccini and D. D. Osheroff, Phys. Rev. B 17, 126 (1978).

[20]G. Eska, K. Neumaier, W. Schoepe, K. Uhlig, W. Wiedemann, and P. Wölfle, Phys. Rev. Lett. 44, 1337 (1980).

[21]G. Eska, K. Neumaier, W. Schoepe, K. Uhlig, and W. Wiedemann, Phys. Lett. 87A, 311 (1982).

[22]T. Kodama and H. Kojima, Phys. Lett. 87A, 103 (1981).

[23]P. Wölfle, Rep. Prog. Phys. 42, 269 (1979).

[24]M. Barmatz and I. Rudnick, Phys. Rev. 170, 224 (1968).

[25]L. Fritsche, Acoustica 10, 189 (1960).

[26]See, e.g., L. D. Landau and E. M. Lifshitz, *Fluid Mechanics* (Pergamon, Oxford, 1959).

[27]J. C. Wheatley, Rev. Mod. Phys. 47, 415 (1975).

[28]P. Wölfle (private communication).

[29]D. G. Carless, H. E. Hall, and J. R. Hook, J. Low Temp. Phys. (in press).

[30]C. N. Archie, Ph.D. thesis, Cornell University, 1978 (unpublished).

[31]J. M. Parpia, Ph.D. thesis, Cornell University 1979 (unpublished).

[32]Y. A. Ono, J. Hara, and K. Nagai, J. Low Temp. Phys. 48, 167 (1982); Y. A. Ono and J. Hara, Physica 107B, 45 (1981).

[33]K. Uhlig, Ph.D. thesis, Technical University Munich, 1982 (unpublished).

[34]G. Eska, K. Neumaier, K. Uhlig, W. Wiedemann, and W. Schoepe, Physica 108B, 1153 (1981).

[35]D. Rainer (private communication).

[36]A. I. Ahonen, J. Kokko, M. A. Paalanen, R. C. Richardson, W. Schoepe, and Y. Takano, J. Low Temp. Phys. 30, 205 (1978).

[37]G. Baym, C. J. Pethick, and M. Salomaa, J. Low Temp. Phys. 36, 431 (1979).